Editors' Suggestion

Hyperfine interaction and electronic spin fluctuation study on $Sr_{2-x}La_xFeCoO_6$ ($x = 0, 1, 2$) by high-resolution backscattering neutron spectroscopy

T. Chatterji,[1,*] B. Frick,[1] M. Zamponi,[2] M. Appel,[1] H. S. Nair,[3] R. Pradheesh,[4] G. R. Hariprya,[4] V. Sankaranarayanan,[4] and K. Sethupathi[4]

[1]*Institut Laue-Langevin, 71 Avenue des Martyrs, CS 20156, 38042 Grenoble Cedex 9, France*

[2]*Jülich Centre for Neutron Science at Heinz Maier-Leibnitz Zentrum, Forschungszentrum Jülich GmbH, D-85748 Garching, Germany*

[3]*University of Texas El Paso, 500 W. University Avenue, El Paso, Texas 79968, USA*

[4]*Department of Physics, Low Temperature Physics Lab, Indian Institute of Technology Madras, Chennai 600036, India*

(Received 12 March 2018; revised manuscript received 22 June 2018; published 27 September 2018)

The study of hyperfine interaction by high-resolution inelastic neutron scattering is not very well known compared to the other competing techniques viz. nuclear magnetic resonance, Mössbauer, perturbed angular correlation spectroscopy, etc. Also, studies have been limited mostly to magnetically ordered systems. Here, we report such a study on $Sr_{2-x}La_xFeCoO_6$ ($x = 0, 1, 2$) of which the first (Sr_2FeCoO_6 with $x = 0$) has a canonical spin-glass state, the second ($SrLaFeCoO_6$ with $x = 1$) has a so-called magnetic glass state, and the third (La_2FeCoO_6 with $x = 2$) has a magnetically ordered ground state. Our present study revealed a clear inelastic signal for $SrLaFeCoO_6$, a possible inelastic signal for Sr_2FeCoO_6 below the spin freezing temperatures T_{sf}, but no inelastic signal at all for the magnetically ordered La_2FeCoO_6 in the neutron-scattering spectra. The broadened inelastic signals observed suggest hyperfine field distributions in the two disordered magnetic glassy systems, whereas the absent inelastic signal for the third compound suggests no, or a very small, hyperfine field at the Co nucleus due to Co electronic moment. The hyperfine splitting on the Co nucleus is induced by the electronic spin state of the magnetic sample atom, and our experiments add information concerning the timescale of electronic spin fluctuations by the appearance of quasielastic broadening in the μeV range at low Q and spin freezing on the nanosecond timescale below T_{sf}. Whereas these features are observed at low Q for $x = 0$ and 1, they are absent for La_2FeCoO_6, which evidences a gradual increase of the elastic intensity only at large Q near an emerging Bragg peak. Thus both electronic magnetic spin freezing and inelastic excitations arising from nuclear hyperfine splitting at the Co site consistently indicate a different behavior for $x = 2$.

DOI: 10.1103/PhysRevB.98.094429

I. INTRODUCTION

The study of hyperfine interactions by high-resolution inelastic neutron scattering [1] has been well established by now. However, the scientific communities are much less familiar with this technique than they are with Mössbauer, nuclear magnetic resonance (NMR), μSR, and other techniques. Inelastic neutron spin-flip scattering probes the hyperfine field at the nucleus and is limited by the cross section and nuclear spin to a certain number of magnetic atoms of which a handful have been studied [2–9] up to now, such as V, Co, Nd, and Ho. Similar selection limits also exist for the competing Mössbauer and NMR techniques.

Thus far the study of hyperfine interactions by high-energy-resolution neutron scattering has mainly been applied to magnetically long-range ordered materials. To our knowledge, structural disorder was addressed rarely except in an early study of ferromagnetic amorphous CoP_x alloys, where the influence of occupational disorder in the nearest-neighbor shell of Co on the hyperfine field split spectra was studied [2]. Whereas hyperfine splitting (hfs) shows up in high-resolution backscattering as a resolution limited triplet peak structure, centered symmetrically around zero-energy transfer, it was shown in Ref. [2] that a phosphorous concentration dependent distribution of hyperfine fields leads to a broadening of the inelastic excitations observable with neutron backscattering (see Supplemental Material (SM) [10] for further explanations on hfs).

We investigate here two other categories of magnetically disordered materials, a canonical spin glass and a so-called magnetic glass, by high-resolution inelastic neutron backscattering. The existence of hfs in short-range ordered magnetic systems has not been clarified. Naively, one could perhaps imagine to observe no inelastic signal from such materials due to an absent or zero-averaged local field or, alternatively, one could expect a quasielasticlike signal, which may arise due to extreme field distributions induced at the nuclei from the magnetic ions having different environments (a similar observation of quasielasticlike scattering instead of sharp inelastic lines was made on disordered systems with rotational tunnel splitting [11]). This may be the case for some disordered magnets. Also, since this technique essentially probes the magnetic field at the nucleus due to the ordered electronic moment, one expects for magnetically ordered systems to observe an inelastic hfs signal as soon as the atomic spins are frozen and the local field is high enough. At higher temperatures, where the electronic spins are mobile and the field at the nucleus averages to zero, we expect to observe

*Corresponding author: chatterji@ill.fr

no signal for disordered magnets, similar to magnetically ordered materials above T_c. But if the electronic spins of such disordered magnets freeze below a certain temperature, named spin freezing temperature T_{sf}, the residual magnetic moment at the nuclear site may be strong enough that one may expect to observe hfs. As mentioned, the inelastic signal may possess finite broadening due to field distributions [2].

Apart from hfs, inelastic neutron scattering is known to detect electronic spin fluctuations as quasielastic broadening of the elastic line if their electronic spin fluctuation or relaxation time τ_r is shorter than the corresponding spectrometer resolution. For the neutron backscattering spectrometers with finer than 1 μeV full-width energy resolution discussed here, this might be detected for τ_r being shorter than about 2 ns. For longer relaxation times, the measured signal will be elastic, and measuring the temperature dependence of the energy-resolved elastic scattering by elastic fixed window scans (efws) can thus reveal electronic spin freezing. For multiatomic samples as studied here, the quasielastic scattering can potentially arise from spin fluctuations in the electronic environment of any atom and mainly at low Q due to the magnetic form factor.

Double perovskite materials $A_2BB'O_6$ (A = Alkaline earth or rare earth ions; B, B′ = transition metal ions) have drawn intense interest in the condensed matter and materials science community. There are several interesting aspects about these materials viz. antisite disorder, competing magnetic interactions and transition metal spin-state transitions. Antisite defects in double perovskites are related with the magnetoresistance observed in these materials [12]. They also contribute to the competing exchange interactions that lead to frustration and the spin-glass state [13]. The existence of different spin states of B and B′ influences the Jahn-Teller effect. The $A_2BB'O_6$ materials are also reported to show multiferroicity [14] and magnetocapacitance [15], making them truly multifunctional materials.

We have chosen here the class comprising of the series Sr_2FeCoO_6, $SrLaFeCoO_6$, and La_2FeCoO_6. Amongst these, Sr_2FeCoO_6 has been shown to be a canonical *spin-glass* system [16,17], whereas $SrLaFeCoO_6$ can be termed as the so-called *magnetic glass* [18]. There exists no well-defined definition of a *magnetic glass* so far. However, from detailed magnetization experiments, it has been found that these systems have spin disorder and a spin freezing temperature like canonical spin glasses but lack several other typical canonical spin-glass properties. The name magnetic glass has been used for these disordered magnetic systems such as SrLaFeCoO6 [18]. The last member La_2FeCoO_6 becomes *magnetically ordered* [19] below about 225 K. The main aim of our present study concerns the search by neutron backscattering for possible hfs at the Co site, which gives important local information about the electronic magnetism of different selected systems. Another aspect of our investigations is that in addition to the locally induced hfs at the Co site, we exploit the information regarding the electronic spin fluctuations from the same experiment, and from other magnetic atoms in the sample. The momentum transfer and temperature dependence of the elastic and quasielastic scattering reveals interesting information about the electronic magnetism in these systems, which should incite further studies.

II. EXPERIMENTAL

Powder samples of Sr_2FeCoO_6, $SrLaFeCoO_6$, and La_2FeCoO_6 were prepared by a sol-gel method [16] and about 3 g of material were placed in Al sample holders, which were fixed either to the cold tip of the top loading closed-cycle cryostat or in a cryofurnace.

High-resolution inelastic-neutron-scattering experiments were carried out on two different backscattering spectrometers, SPHERES [20], operated by Jülich Center for Neutron Science at the MLZ in Garching, Germany, and IN16B [21,22] at the Institut Laue-Langevin, Grenoble. On both instruments, the wavelength of the incident neutrons is $\lambda = 6.271$ Å with an energy resolution of FWHM $\approx$ 0.7 ± 0.05 μeV in their standard configurations with Si 111 backscattering crystals, a momentum transfer (Q) range between $0.2 < Q < 1.9$ Å^{-1} and the maximum energy transfer near 30 μeV. For most measurements, the energy range was deliberately restricted to the range where the hfs is expected which optimized the count rate. For more instrumental details, see the SM [10].

III. RESULTS

Out of the three samples measured on the two backscattering spectrometers, only the *magnetic glass* sample, $SrLaFeCoO_6$ [18], showed the inelastic signal expected for hfs of the Co nuclear ground state at low temperatures and this is why we will present first the results for this sample even though its electronic magnetic state seems to be more complex [18]. We observe for $SrLaFeCoO_6$ clear inelastic peaks arising from the hfs, which move toward the central elastic line with increasing temperature and finally merge with it near the spin-freezing temperature $T_{sf} = 75$ K. In the same temperature range, the elastic line intensity decreases with increasing temperature for small Q, indicating that electronic spin fluctuations become faster than the resolution timescale.

The second sample, the canonical *spin glass* Sr_2FeCoO_6, showed magnetic excitations at low temperatures as well; however, of less clear nature. This is why we have measured this sample extensively in different instrument configurations to determine if the observed scattering for this sample is quasielastic or inelastic. The elastic line intensity decreases again for small Q with temperature, but the effect is much weaker. Additional quasielastic scattering from spin fluctuations is observed for this sample.

Curiously the last sample, La_2FeCoO_6, which seems to be *magnetically ordered* below about $T = 225$ K, as evidenced from neutron diffraction experiments [19], did not show any measurable inelastic nor quasielastic signal in the whole temperature range up to 300 K. For this sample, the elastic line intensity does not change with temperature at small Q, but evidences a continuous increase below 225 K at high Q near some additional Bragg peak.

A. Magnetic glass $SrLaFeCoO_6$

According to neutron powder diffraction, $SrLaFeCoO_6$ has a monoclinic (space group: $P2_1/n$) crystal structure, which is retained without phase transition down to 4 K, yet with some weak changes in the temperature dependence of the unit cell

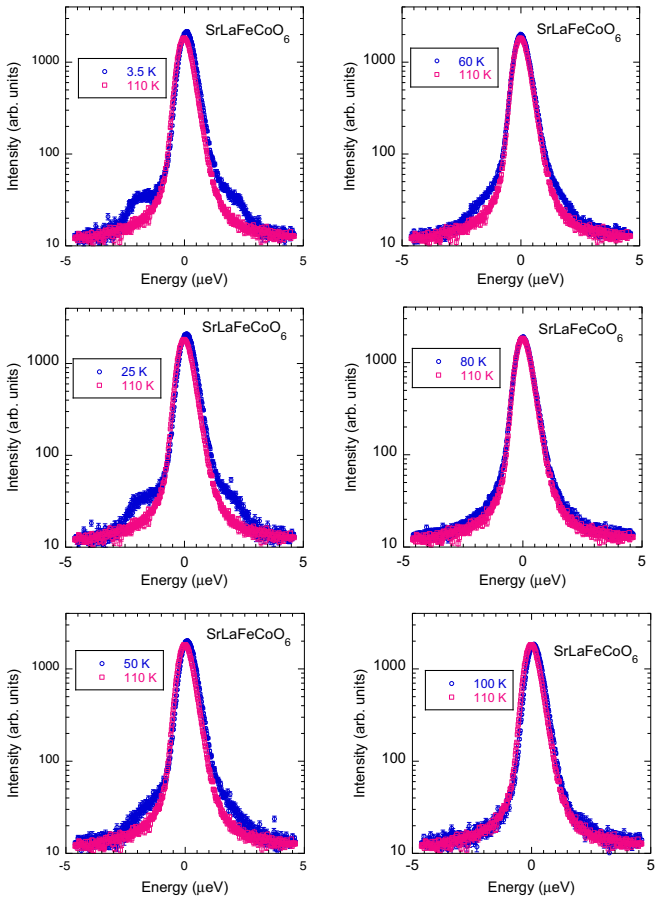

FIG. 1. Neutron spectra from $SrLaFeCoO_6$ at several temperatures compared to the spectrum at $T = 110$ K measured on SPHERES. There exists extra inelastic scattering at low temperatures below the spin temperature $T_{sf} \approx 75$ K. The inelastic excitation is located at an energy of about 1.8 μeV and moves toward the central elastic peak with increasing temperature, merging at about the spin-freezing temperature T_{sf}.

volume near $T = 250$ K and 75 K. No long-range magnetic order is observed in the neutron powder diffraction patterns [18]. However, unusual features in magnetization measurements resemble a kinetic arrest near $T_{sf} \approx 75$ K, which led Pradheesh *et al.* to classify $SrLaFeCoO_6$ as a so-called *magnetic glass* [18] below the spin freezing temperature T_{sf}.

From our backscattering spectroscopy on $SrLaFeCoO_6$, we show first the temperature dependence of the spectra in comparison to a spectrum measured at $T = 110$ K, which serves as a measurement of the resolution (see Fig. 1). Another data set from IN16B, showing the temperature dependence of the hfs splitting with somewhat better resolution, can be found in Sec. III of the SM, Fig. 1 [10]. Spectra were always summed over a large detector range because no dispersion was found within the limits of the present statistics of single detectors. We observe inelastic scattering below the spin freezing temperature $T_{sf} \approx 75$ K, which is located at an energy of about 1.8 μeV at $T = 3.5$ K moves with increasing temperature toward the central elastic peak, finally merging with it near T_{sf}. The fit results for the temperature dependence of the inelastic peak positions are shown in Fig. 2,

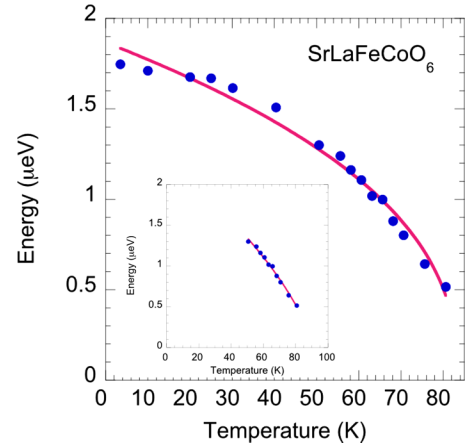

FIG. 2. Power-law fit to the temperature dependence of the energy of hyperfine splitting in $SrLaFeCoO_6$: fit in which equal widths of the inelastic peaks were fixed to the low temperature value. Fits for all data are shown in the main figure whereas the inset shows fits above $T = 40$ K only.

and details of the fits to the SLFCO spectra are described in the SM [10]. Without attributing too much significance to the functional, the temperature dependence of the average hfs can be parameterized by power laws (another example is shown in the SM, Fig. 3) with fit parameters which slightly depend on the way the spectra are fitted. Correspondingly, magnetic transition temperatures of $T_{sf} = 71.1 \pm 0.8$ K and $T_{sf} = 83 \pm 1$ K were obtained [10].

Besides the peak position, the peak width may carry information on disorder if they are broadened beyond the resolution width. To investigate this point, we repeated measurements of $SrLaFeCoO_6$ on IN16B, exploiting the high signal-to-noise ratio (HSNR) mode [23] and a better separation of the excitations from the elastic resolution wing. This higher sensitivity allows for a more detailed discussion of the model fits [24] of the hyperfine split spectra. We show in Fig. 3 (and in the SM, Fig. 4 [10]) the spectra measured at $T = 2$ K

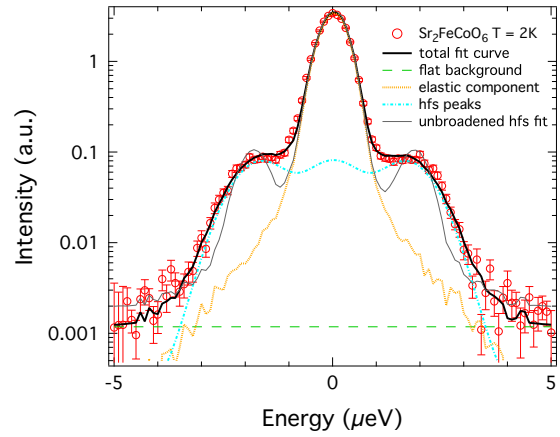

FIG. 3. Fit of the SLFCO spectrum at $T = 2$ K (total fit: thick black line) with a broadened hyperfine spectrum (dash-dotted line), additional elastic component (dotted), and flat background (dashed). Without a broadening of the hyperfine spectrum the total fit shows too sharp features (thin solid line). Experimental data are summed between Q = 0.5 and 1.87 $Å^{-1}$.

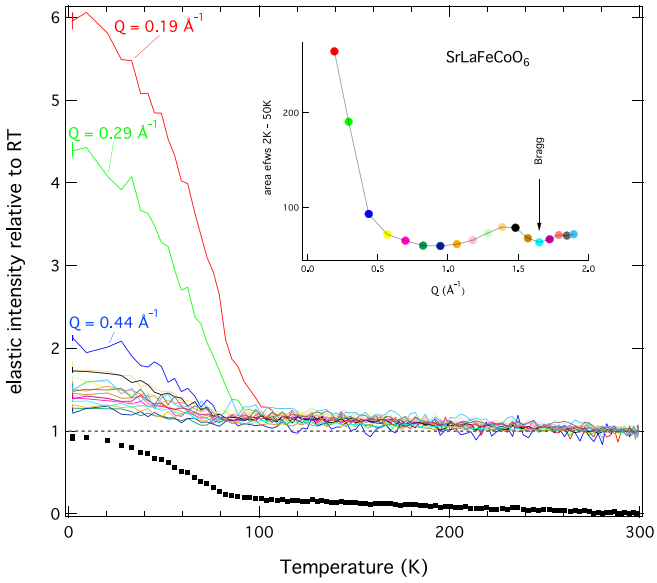

FIG. 4. Temperature-dependence of the elastic intensity of $SrLaFeCoO_6$ normalized to its high-temperature average value, measured on the backscattering spectrometer IN16B. Main panel, bottom (black squares): sum over all Q-values; for clarity offset by -1. Lines in the main panel: elastic intensity for different Q values, with the three lowest Q-values labeled. A strong increase of the elastic intensity is observed at low Q for temperatures below $T = 80$ K. The inset displays the Q dependence of the integrated intensity ("area") between $T = 2$ and 50 K for these curves, where the colors of the symbols in the inset correspond to the line colors of the curves in the main panel. Besides the low temperature intensity increase at low Q, another small relative intensity increase of an elastic diffuse contribution can be observed below the high-temperature Bragg peak position (indicated by an arrow) at $Q = 1.57$ Å^{-1}. Note that the intensities are scaled to $T = 300$ K.

and the corresponding model fits for $SrLaFeCoO_6$. These data were averaged over Q values between $Q = 0.57$ and 1.87 Å^{-1}. The spectrum is well fitted by a single hfs spectrum (thick solid black line in Fig. 3; $\chi^2 = 1.88$) with a ground-state level splitting of 1.67 ± 0.05 μeV (consistent with fits of the spectra shown in SM, Fig. 3 [10]), an additional elastic contribution as well as an additional weak flat background (two orders of magnitude lower than the inelastic peak height). These fits reveal a clear broadening of the hyperfine split lines (Gaussian $\sigma \approx 0.715 \pm 0.018$ μeV), whereas the theoretically expected nonbroadened delta function triplet for hfs does not describe the spectra well (shown as a thin solid black line in Fig. 3). A justification for fitting broadened lines can easily be found in the magnetic short-range order, which is ascribed to site disorder in these perovskites [18]. A broadening of hyperfine split lines had been observed by Heidemann [2] in early studies of disordered Co alloys. We have also tried an alternative fitting model (SM, Fig. 4 [10]) fixing the hyperfine spectrum to resolution width, but adding a quasielastic Lorentzian component. The motivation for trying such a fit will become more clear below. This fit is somewhat worse ($\chi^2 = 4.5$) and results in hyperfine peaks which are too sharp.

Finally, we discuss the temperature dependence of the intensities. The nuclear spin excitations observed at low temperature arise from inelastic spin flip scattering on a nuclear ground state which is split by a local magnetic field (Sec. I, SM [10]). However, incoherent spin-flip scattering exists, of course, as well at high temperature in the absence of such a field and therefore without ground-state splitting. The corresponding incoherent intensity is then contained in the elastic line because there is no energy exchange related with the spin-flip scattering process. Thus, if we follow the temperature dependence of the elastic intensity, we expect to see with decreasing temperature near T_{sf} for this scattering contribution a transfer from elastic to inelastic intensity and therefore a decrease, which is estimated for our sample to be on the 1% level. Other contributions to the elastic line are isotope incoherent scattering, coherent nuclear scattering, and electronic magnetic scattering contributions. Therefore, unlike earlier studies, we have investigated the temperature dependence of the energy resolved elastic intensity by efws (Fig. 4). With decreasing temperature, the Q-averaged elastic intensity shows a pronounced increase below $T \approx 80$ K, shown in Fig. 4 in the lower part of the main panel. Cooling down from 300 K, the average elastic intensity increases initially weakly and then rises near 80 K by nearly 60%. A glance at the individual Q values reveals that the elastic intensity increase is most pronounced in the low Q region (colored lines in the main panel of Fig. 4) where, e.g., at $Q = 0.19$ Å^{-1} the elastic intensity increases by nearly 600%. The onset temperature is about 100 K for low Q-values and about 80 K for high Q. The Q-dependence of this low temperature elastic intensity increase is displayed in the inset of Fig. 4, where for each Q the intensity (relative to its high temperature value) was integrated between 2 K and 50 K (called "area"). This shows clearly that the elastic intensity increase is strongest at low Q, resembling an electronic magnetic form factor. In addition, we observe at higher Q elastic diffuse scattering, around the first structural Bragg peak position. Such a temperature behavior of the elastic intensity below T_{sf} does not correspond to a hyperfine interaction which is supposed to be Q-independent but from its Q-dependence must rather be interpreted as the onset of electronic magnetic scattering, which is static at the ns timescale below T_{sf}. The apparently higher onset temperature observed for low Q data might simply arise from stronger magnetic intensities due to the higher magnetic form factor at low Q. Consistent with earlier neutron diffraction results, we find no magnetic reflections [18], but we observe signs of magnetic short-range order and electronic spin freezing between $T \approx 80 - 100$ K. The existence of spin fluctuations or spin dynamics is further confirmed when analyzing full energy spectra near T_{sf} which are discussed in the Appendix A. Thus, whereas further experiments and techniques are needed to fully exploit the electronic magnetism, it is certainly helpful to include here at least a qualitative discussion of the observed spin freezing as it is certainly inducing the hfs at the Cobalt nucleus—indicated in our experiment by the onset of both effects in the same temperature range.

B. Canonical spin-glass sample Sr_2FeCoO_6

Neutron powder diffraction and bond valence sums analysis for Sr_2FeCoO_6 has shown that the B site in this double perovskite is randomly occupied by Fe and Co in mixed valence

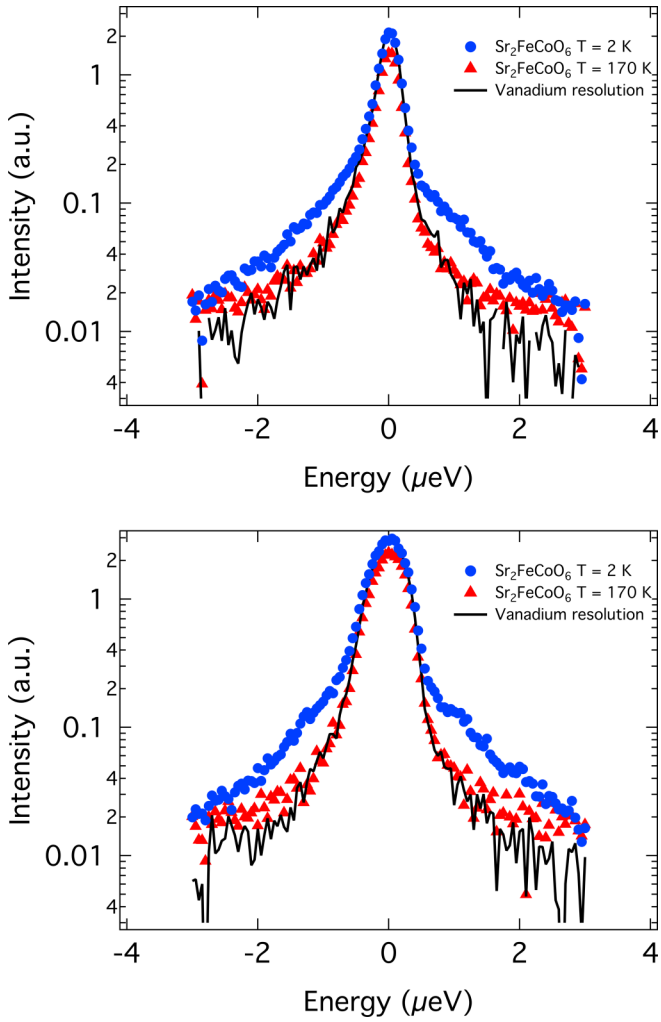

FIG. 5. Spectra of Sr_2FeCoO_6 measured on IN16B with higher energy resolution: (a) top spectra summed in the lower Q range and resolution of FWHM ≈ 0.31 μeV and (b) bottom: at higher Q values with the "unpolished" analyzers (see text) and a resolution of FWHM ≈ 0.6 μeV. At $T = 2$ K one sees clearly the signal from hyperfine splitting, whereas at $T = 170$ K the linewidth is identical with the measured Vanadium resolution, which is scaled to the elastic peak intensity of the sample at 2 K.

states of Fe^{3+}/Fe^{4+} and Co^{3+}/Co^{4+}, respectively [16]. The resulting competition of ferromagnetic and antiferromagnetic interaction leads to a spin-glass phase with a freezing temperature of $T_{sf} \approx 80$ K [16]. Detailed magnetization studies [16] have shown that Sr_2FeCoO_6 can be considered a canonical spin glass. High-resolution neutron-diffraction investigations [19] did not show any appreciable magnetic Bragg scattering down to a temperature of about 10 K.

When searching for hfs of Cobalt in Sr_2FeCoO_6, weak indications for extra scattering at $T = 3.5$ K compared to $T = 150$ K were found on the backscattering spectrometer SPHERES (shown in Fig. 5 of the SM [10]), which did not allow us to fit the hfs. However, hfs is clearly confirmed by higher resolution measurements on IN16B, when comparing the 2 K spectrum of Sr_2FeCoO_6 with both a Vanadium resolution and a $T = 170$ K Sr_2FeCoO_6 spectrum (see Fig. 5). The spectra in Fig. 5 were measured with narrower energy resolution and a reduced energy-transfer range of ± 3 μeV to improve statistics. The top spectra were added in the Q range from 0.44–1.06 $Å^{-1}$ and the fitted energy resolution for Vanadium was 0.31 μeV. The spectra in the bottom figure were added in the Q range from 1.06–1.8 $Å^{-1}$ and the fitted energy resolution was ≈ 0.6 μeV (see SM, Sec. II for more instrumental details [10]). The symmetric shoulders on both sides of the elastic line in the spectra depicted in both figures for $T = 2$ K suggest that there is inelastic low-frequency scattering from hfs. At the chosen high reference temperature, $T = 170$ K, the electronic spins fluctuate randomly and the Sr_2FeCoO_6 spectrum corresponds well to the Vanadium resolution.

Nevertheless, without model fitting, it cannot be decided safely if the observed extra scattering is inelastic or quasielastic. As hfs for spin glasses has not yet been reported, we put some more emphasis on the data fitting [24] of Sr_2FeCoO_6 and discuss now different fit models: For a canonical spin glass below the spin-freezing temperature T_{sf}, one may expect a distribution of hyperfine fields and therefore a broadening of the inelastic scattering, similar to what was reported above for $SrLaFeCoO_6$. For a very broad distribution, this could resemble quasielastic scattering, in analogy to what was reported for quantum rotational tunneling [11] in disordered systems. The 2 K spectrum in the top panel of Fig. 5 was fit in different ways: A, by a typical hfs consisting of a symmetric triplet of resolution convoluted delta functions; B, by a quasielastic Gaussian centered at $E = 0$; and, finally, C, by a quasielastic Lorentzian centered at $E = 0$. Figure 6 shows fits for models A and B, whereas fits for model C are not shown.

Model A. A good description by the most plausible hfs fit function [1] was only possible if additional Gaussian broadening of the hfs peaks due to disorder was assumed. The three Gaussians were constrained to be symmetrically positioned and of equal width and intensity, as shown in Fig. 6 on the left hand side. The reasoning behind this fit function is like above for $SrLaFeCoO_6$, that the local induced field at the Cobalt site of the spin glass Sr_2FeCoO_6 is heterogeneous due to disorder and that the hfs lines are correspondingly broadened. The fits indicate a hfs energy splitting, which amounts only to about 1 μeV.

As for the temperature dependence of the hfs in Sr_2FeCoO_6, we find the typical scenario (see SM, Figs. 5 and 6) [10], i.e., softening of the side peak positions with increasing temperature and finally merging with the elastic line at the magnetic transition temperature, like for the magnetic glass $SrLaFeCoO_6$. For temperatures between 2 K and 60 K, the spectra hardly change, but near 70 K the intensity in the wings diminishes as a first sign of softening and finally, near $T_{sf} =$ 85 K or slightly above, the inelastic peaks have merged into the elastic line. The fit quality with the broadened hfs model A (shown in Fig. 6 for 2 K) is excellent for all spectra below $T = 70$ K with an average $\chi^2 = 1.3 \pm 0.13$. The resulting fit parameters for fits with model A, like the temperature-dependent peak positions, the width and the intensity, are shown in the SM, Fig. 7 [10]. Another attempt to fit the spectra with two different sets of hfs lines is discussed in Sec. III B of the SM [10].

Model B. A fit with a centered quasielastic Gaussian would be another reasonable description of the underlying physics

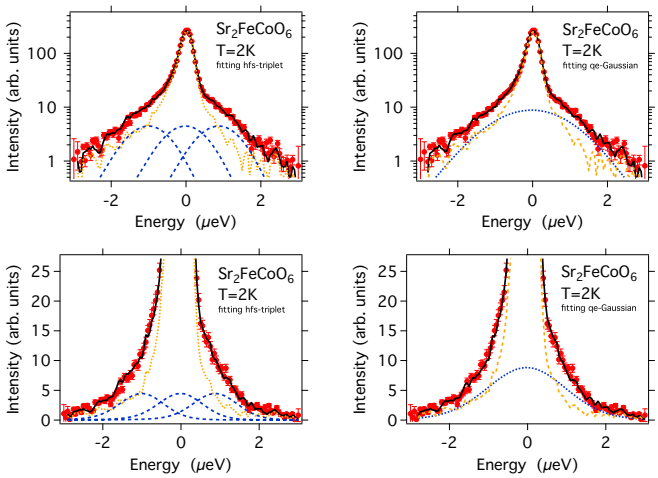

FIG. 6. Fits of the spectra of Sr_2FeCoO_6 at $T = 2$ K, measured on IN16B with high-resolution (FWHM = 0.3 μeV) polished Si111 setup. Spectra were summed between Q = 0.44 and 1.06 Å^{-1}. The upper figures are in log scale in intensity and the lower figures are in linear scale. The black line through the data points (red symbols) is a fit of the total model curve convoluted with the Vanadium resolution function. The dotted yellow line results from a fit of the additional dominating elastic scattering convoluted with the resolution and the blue dashed lines represent the subfunctions used to describe the additional inelastic and quasielastic scattering. Left column: a typical scattering law for nuclear hfs results in a triplet of equidistant (elastic + symmetric inelastic) delta functions of same intensity, convoluted with the instrumental resolution. Here we had to assume, in addition, a Gaussian broadening of the triplet functions in addition to the convolution with the resolution. Right column: Fit with a single, zero energy entered, Gaussian function convoluted with the resolution function (blue dotted line) and the dominant elastic scattering (yellow dotted line).

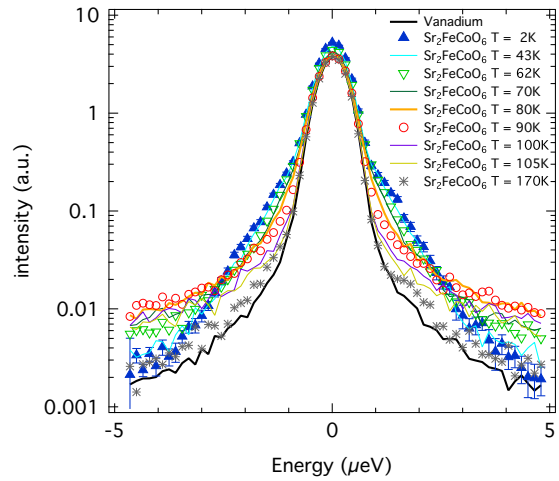

FIG. 7. Temperature dependence of the Sr_2FeCoO_6 spectra between 2 K and 170 K compared to the Vanadium resolution (summed from Q = 0.65 Å^{-1} to 1.9 Å^{-1}). Due to a factor 10 improved signal-to-noise ratio of the IN16B HSNR mode and the energy range extending to 5 μeV compared to Fig. 5, the presence of additional quasielastic scattering between $T = 62$ K and 170 K becomes clear.

if the distribution of local fields at the Co site and thus the local hfs would average to $E = 0$. The width of the Gaussian is related to the width of the assumed Gaussian distribution. The fit quality of this model is equally good with an average $\chi^2 = 1.28 \pm 0.13$ below $T = 70$ K (Fig. 6, right hand side). Within the investigated energy range, the linewidth of the Gaussian results to be decreasing with temperature (see SM, Fig. 8) [10]. The area of the Gaussian function remains about constant below 70 K and then decreases quickly within 20 K. In this model, a decreasing width would mean that the distribution of the local hfs becomes narrower with increasing temperature.

Model C. Fitting a centered quasielastic Lorentzian function could be based on relaxation of the nuclear or possibly even the electronic spins. Again such fits are relatively good for temperatures below $T = 70$ K (not shown) though $\chi^2 = 1.44 \pm 0.14$ is slightly higher. Again the width of the central Lorentzian becomes narrower with increasing temperature (from a FWHM of 1.84 ± 0.18 μeV at 2 K to a FWHM of 1.22 ± 0.12 μeV at 80 K) and its fitted intensity disappears above 85 K. However, as this model is based on relaxations, a narrowing of the width with temperature would mean a slowing down of the relaxations with increasing temperature, which we judge to be unphysical.

We have then remeasured Sr_2FeCoO_6 spectra at selected temperatures with better signal-to-noise on IN16B (in the HSNR mode [23]) and have extended the energy transfer

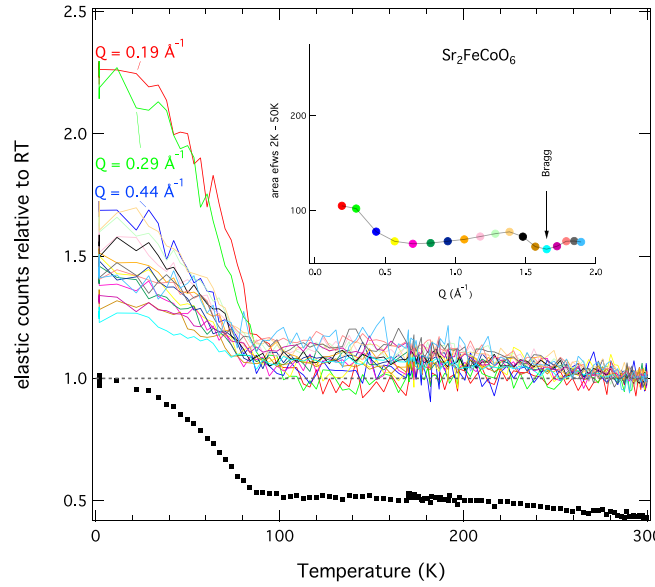

FIG. 8. Temperature-dependence of the elastic intensity of Sr_2FeCoO_6 normalized to its high temperature average value for all Q values measured. Main panel, bottom (black squares): sum over all Q values; for clarity offset by −0.57. Lines in main panel: elastic intensity for different Q values. A strong increase of the elastic intensity is observed below $T = 80$ K. Inset: The Q dependence of the area under the efws curves between $T = 2$ and 50 K, where the colors of the symbols in the inset correspond to the line colors of the curves in the main panel. Besides the low temperature intensity increase at low Q, another small relative intensity increase of an elastic diffuse contribution can be observed below the high temperature Bragg peak position (indicated by an arrow) at Q = 1.65 Å^{-1}. Note that the intensities are scaled to $T = 300$ K.

range to ±5 and ±30 μeV respectively, with the aim to search for possible quasielastic scattering. At $T = 2$ K a comparison with the Vanadium resolution function (Fig. 7) or a comparison of spectra for both samples, Sr_2FeCoO_6 and $SrLaFeCoO_6$ (shown later in Fig. 12) evidence clearly that we observe an inelastic signal. With increasing temperature, we find for energies below 3 μeV a narrowing of the spectra, consistent with the high-resolution measurements above. However, further out in energy transfer this narrowing goes along with an increase of the spectral intensity in the range 3–5 μeV. This intensity increase reaches a maximum near the transition temperature $T \approx 80$–90 K before decreasing again to the level of the low temperature spectrum, which is a strong indication of the presence of additional quasielastic scattering which broadens with temperature. Whereas the temperature behavior, i.e., a softening of the hfs and the onset of quasielastic scattering near T_{sf} is qualitatively similar to $SrLaFeCoO_6$ (Fig. 14), it is different in that the quasielastic scattering is now observed as well for high Q values. The energy window of ±3 μeV chosen previously with the high-energy resolution setup was too narrow and the signal-to-noise ratio insufficient to detect this intensity increase. Both measurements together, however, evidence the existence of hfs, which softens near the transition temperature simultaneously with the uprising of quasielastic scattering.

Whereas a more detailed investigation of the quasielastic scattering is needed, these measurements show that the hfs splitting is best fitted at the lowest temperature where a quasielastic contribution is absent and at higher temperatures this quasielastic scattering needs to be taken into account when fitting the hfs spectra for the spin glass Sr_2FeCoO_6.

We have argued above that the elastic intensity reveals the temperature behavior of the electronic magnetism, which is related to the onset of hfs. This is why we have investigated similarly the temperature and Q dependence of the elastic intensity for the spin glass Sr_2FeCoO_6. Qualitatively, we find in cooling the same behavior as reported above for $SrLaFeCoO_6$ with a slow intensity increase between 300 K and 100 K and a steep increase near T_{sf} toward low temperatures as shown in Fig. 8. The Q dependence of the elastic intensity rise at low temperature (inset to Fig. 8) is again most pronounced for lowest Q values, and again we observe a diffuse peak below the high-temperature Bragg peak position.

C. Magnetically ordered La_2FeCoO_6

High-resolution neutron diffraction studies showed that La_2FeCoO_6 orders [19] magnetically below about 225 K and that there is also a structural transition at the same temperature. Simulation work predicts a ferromagnetic semiconductor state [27,28] without specifying a transition temperature.

However, to our surprise, in spite of this magnetic ordered state, we observe for La_2FeCoO_6 down to 1.8 K no measurable quasi- or inelastic signal on both backscattering spectrometers. The spectra taken on SPHERES at four different temperatures are shown in Fig. 9, and additional measurements on IN16B using the high-resolution configuration and comparing the spectra at 2 K with Vanadium within a ±3 μeV energy window (see SM, Fig. 10) or comparing with a 250 K spectrum (see Fig. 10) over an extended energy range of

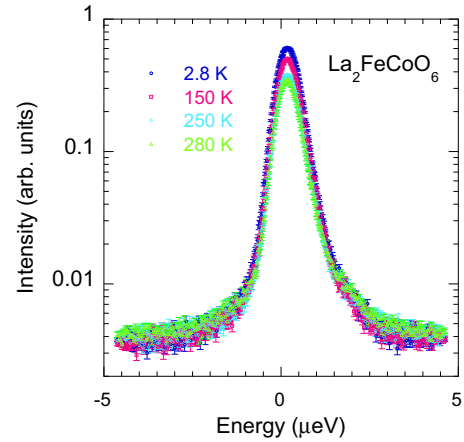

FIG. 9. Spectra of La_2FeCoO_6 at different temperatures. There exist no extra scattering at low temperatures.

±30 μeV (Fig. 10) confirm this observation. Only the elastic intensity has decreased between 2 K and 250 K.

Thus data from both instruments indicate that there might be a background increase with temperature, but no sign of an inelastic hfs. The implication of this negative result is obviously that the hyperfine field at the Co nuclear site is too weak and that the magnetic moments of Co ions may not get ordered or frozen at low temperatures. But since we probe only locally the hfs on the Cobalt site. We cannot exclude an ordering of Fe spins.

Finally, we have as well analyzed the elastic scattering for La_2FeCoO_6 by efws as function of temperature. Raw data as a function of Q and T are shown in the Appendix B, Fig. 15 as a 3D plot. In cooling, we see clearly that an additional Bragg peak emerges in the high Q-range below the Bragg peak position of the high-temperature phase ($Q \approx 1.65$ Å^{-1}), though we cannot say if its origin is nuclear or magnetic.

In Fig. 11, we illustrate the relative elastic intensity increase during an efws in cooling with respect to 250 K. In

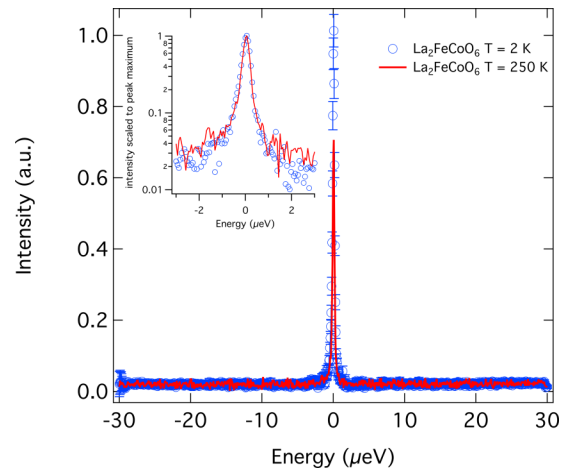

FIG. 10. Spectra of La_2FeCoO_6 measured on IN16B with higher resolution and over a wider energy transfer range. The data are plotted on a linear intensity scale and are not normalized. The inset shows the near elastic region on a logarithmic intensity axis scaled to peak maximum.

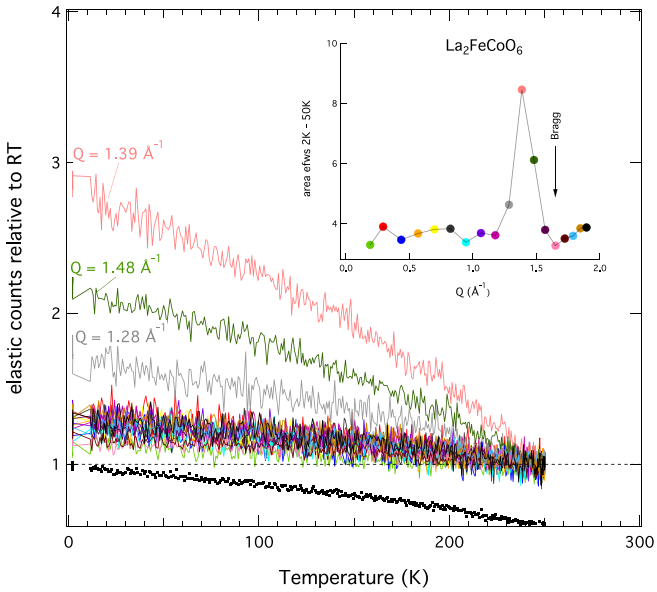

FIG. 11. Temperature-dependence of the elastic intensity of La_2FeCoO_6 normalized to its high temperature average value. Main panel, bottom (black squares): sum over all Q values; for clarity offset by −0.6. Lines in the main panel: elastic intensity for different Q values, with the three Q values of the low-temperature Bragg peak labeled. Besides, at the additional Bragg peak the elastic intensity increases only weakly with decreasing temperature. Inset: The Q dependence of the area under the efws curves between $T = 2$ and 50 K, where the colors of the symbols in the inset correspond to the line colors of the curves in the main panel. No additional increase at low Q is observed, only the appearance of an additional Bragg peak (011) at Q ≈ 1.4 Å^{-1} below the high-temperature Bragg peak position marked with an arrow at Q = 1.61 Å^{-1}. Note that the intensities are scaled to $T = 250$ K.

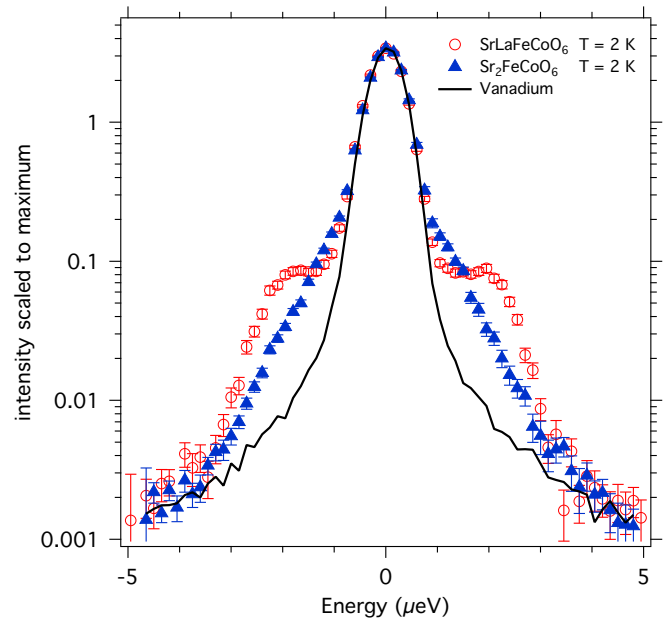

FIG. 12. Comparison of $SrLaFeCoO_6$ (red open circles) and Sr_2FeCoO_6 (blue filled triangles) spectra measured at $T = 2$ K compared to the Vanadium resolution spectrum (line). All spectra are background corrected and summed between Q = 0.44 and 1.9 Å^{-1}. The intensities are normalized to the elastic peak maximum.

contrast to the first two samples discussed, La_2FeCoO_6 orders at high temperature ($T \approx 225$ K) and the elastic intensity increases only gradually without the steplike increase observed for $SrLaFeCoO_6$ and $SrLaFeCoO_6$. This is depicted for the Q-averaged intensity in the lower part of Fig. 11 (black dots) and for the individual Q values (colored lines) in the main panel. Whereas our scans do not start sufficiently far above the supposed transition temperature $T \approx 225$ K to exclude a potential steplike change above, nearly identical spectra observed at 250 K and 280 K on SPHERES (Fig. 9) render this highly improbable. It should be stressed that in Fig. 11, the curves with a stronger relative elastic intensity increase in cooling (labeled with their respective Q values) belong for La_2FeCoO_6 to the high Q range where an additional Bragg peak was found, near Q ≈ 1.4 Å^{-1}. This is seen as well from the inset to Fig. 11, which displays in analogy to Figs. 4 and 8 the Q dependence of the area under the efws curves between $T = 2$ and 50 K.

IV. DISCUSSION

We have presented results from high-energy resolution neutron backscattering on three double perovskite samples of type $A_2BB'O_6$ with B:B′ = 1:1 = Fe:Co where the occupation of the A-site was either complete with La and Sr, respectively, or 1:1 with La:Sr. The three investigated samples have completely different magnetic ground states, which therefore cannot be ascribed to the unchanged B-site disorder alone. From literature it is known that, at low temperature, Sr_2FeCoO_6 is a canonical spin-glass state, $SrLaFeCoO_6$ a magnetic glass, and La_2FeCoO_6 magnetically ordered. Our inelastic-neutron-scattering measurements serve first as a local probe for the hyperfine field which might or not be induced at the Cobalt nucleus by the electronic spins. Second, the additionally investigated temperature dependence of the elastic intensity (efws) reveals changes which stem from the electronic magnetic moments of both the Co and Fe ions, for which besides cation site disorder, a valence state disorder seems to be of importance. A slowing down of electronic spin fluctuations or spin freezing at low temperature shows up in the efws as an intensity increase, whereas the appearance of hfs at low temperatures should rather be reflected in an elastic intensity decrease on cooling, given that the inelastic spin flip scattering separates from the elastic line at low temperature. The efws could in principle be further influenced by structural changes (coherent diffraction contributions) or atomic diffusion (mainly incoherent, but also coherent).

As for the inelastic measurements, we observe for both Sr_2FeCoO_6 and $SrLaFeCoO_6$ extra scattering outside of the resolution which can be ascribed to the existence of hyperfine splitting at the Co site. This is summarized for $T = 2$ K in Fig. 12. $SrLaFeCoO_6$ shows clear inelastic scattering as known for hfs and model fits show that the inelastic peaks are broadened, which we ascribe to disorder in the electronic spin system and thus the field at the Co sites. The spectra for Sr_2FeCoO_6 are significantly narrower, probably due to a weaker local field at the Co nucleus. Finally, for La_2FeCoO_6

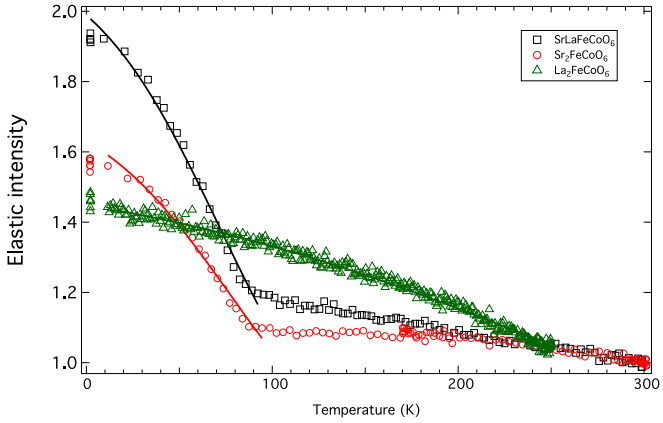

FIG. 13. Elastic intensity of La_2FeCoO_6 (green triangles) measured on IN16B in high-resolution mode summed over all detectors, compared to the elastic intensity of Sr_2FeCoO_6 (red circles) and $SrLaFeCoO_6$ (black squares). The data are normalized to the highest temperatures measured and for La_2FeCoO_6 to the $T = 250$ K value of the others. Lines are fits with Brillouin functions with Tc fixed to 75 K and 250 K.

(Figs. 9 and 10 and SM, Fig. 10) we find no extra inelastic scattering within the applied instrumental resolution range. The temperature dependence of the peak positions of the hfs spectra for both the spin glass Sr_2FeCoO_6 and the magnetic glass $SrLaFeCoO_6$ resemble the conventional hfs behavior of other systems: a softening of the inelastic peak positions is observed with a final merging into the elastic line near the transition temperature (see Fig. 2 and SM, Figs. 3 and 7). In contrast, hardly any change of the inelastic spectra is observed with temperature for the magnetically ordered La_2FeCoO_6.

The temperature dependence of the elastic intensity provides information regarding the electronic magnetism and is summarized for the investigated samples in Fig. 13. For the relative elastic intensity of $SrLaFeCoO_6$ and Sr_2FeCoO_6, which are magnetically disordered, but show signatures of hfs in the inelastic neutron spectra, we find in the efws a clear steplike increase below the spin freezing temperatures known from literature (Fig. 13). In contrast, for the efws of the magnetically ordered La_2FeCoO_6 we observe in cooling only a smooth elastic intensity increase. The onset temperatures of the steplike increase of the elastic intensity for $SrLaFeCoO_6$ and Sr_2FeCoO_6 and the temperatures where the hfs merges into the elastic line roughly coincide. As the appearance of hfs would rather lead to a decrease of the efws near the transition temperature, we postulate that the observed elastic intensity increase is due to an ordering or freezing of the electronic spins, which is at the origin of the hyperfine field at the Co site. That the relative increase of the efws step is smaller for Sr_2FeCoO_6 compared to $SrLaFeCoO_6$ is consistent with an observed smaller hfs or smaller local field at the Co site for Sr_2FeCoO_6.

The Q dependence of the efws provides additional useful information which can be compared to the known diffraction results. For the ordered magnetic system, La_2FeCoO_6, we find in the elastic scattering the known Bragg peaks, particularly the additional Bragg peak appearing below $T \approx 225$ K near $Q \approx 1.4$ Å^{-1}. For the disordered magnetic systems, however, no long-range or short-range magnetic order has been reported. We find at the lowest temperatures, where the electronic spins are assumed to be frozen, in the Q dependence of the efws for both magnetically disordered systems diffuse scattering near $Q \approx 1.4$ Å^{-1}, the region where for the magnetically ordered La_2FeCoO_6 a Bragg peak appears. Furthermore, both $SrLaFeCoO_6$ and Sr_2FeCoO_6 show an increase in the elastic intensity at small Q, which is again most pronounced for $SrLaFeCoO_6$ and not present for La_2FeCoO_6.

Finally, we point out that quasielastic scattering appears near the reported freezing temperatures, which suggests spin fluctuations on the ns timescale. This quasielastic scattering is visible only at small Q for the magnetic glass $SrLaFeCoO_6$, it is visible as well at higher Q for the spin glass Sr_2FeCoO_6, and either missing or too wide for the ordered La_2FeCoO_6. Thus we speculate that with the addition of Sr in $La_{2-x}Sr_xFeCoO_6$ the spin fluctuations may slow down. In La_2FeCoO_6, the spins could be frozen or fluctuate very fast with the corresponding quasielastic signal being wider than the energy range of IN16B. In the magnetic glass also, the fluctuations are probably quite fast too and only visible in the low Q, long-range region and may related to the postulated magnetic domains in this system. Finally, for the spin glass Sr_2FeCoO_6, the fluctuations would be more localized and further slowed down, so that quasielastic scattering becomes visible even at higher Q. At the same time, the complete freezing of spins, related to the relative step height of the efws, would become more rare. We are aware that our data provides no strong support for such speculations and that the real explanation might be much more complex, but at least they demonstrate some trend for an otherwise nonmonotonous behavior of the measured hfs with he La/Sr-ratio. Our measurements might incite a more detailed study of the spin fluctuations in the spin glass Sr_2FeCoO_6.

V. CONCLUSION

We have presented results on the hyperfine field of Cobalt obtained by inelastic neutron scattering for the double perovskites $La_{2-x}Sr_xFeCoO_6$ for $x = 0, 1, 2$ and on a spin glass. An important conclusion from these experiments on Sr_2FeCoO_6, $SrLaFeCoO_6$, and La_2FeCoO_6 is that the first two are magnetically disordered systems and still show hfs, whereas for the magnetically ordered La_2FeCoO_6 system, no hf-splitting is observed. This observation does not conform with changes controlled in proportion to the Sr concentration x, and indicates that the effect of A-site doping in $AA'FeCoO_6$ is more complex. The same is valid in what concerns the temperature and Q dependence of the elastic intensity, for which a steplike increase at low temperatures is interpreted as freezing of the electronic spin fluctuations. The relatively strong spin fluctuations observed for the spin glass Sr_2FeCoO_6 require further investigation and our measurements may incite further studies on this interesting class of double perovskites.

ACKNOWLEDGMENTS

The present work is based upon experiments performed on IN16B at ILL, Grenoble, France and also on the Spheres

instrument operated by the Juelich Center for Neutron Science at the Heinz Maier-Leibnitz Zentrum (MLZ), Garching, Germany. T.C. gratefully acknowledges the financial support provided by Juelich Center for Neutron Science to perform experiments at MLZ, Garching, Germany.

APPENDIX A: $SrLaFeCoO_6$

Here we investigate the Q and temperature dependence of the elastic and inelastic intensity using spectra of $SrLaFeCoO_6$ measured on IN16B, as shown in Sec. III A of the SM [10]. We will show that for this data set, we could detect the onset of quasielastic scattering at low Q when integrating different spectral ranges. The temperature dependence of the intensity within different energy windows is shown in Fig. 14 for the three lowest investigated Q values. The total intensity (within ± 5 μeV) increases with decreasing temperature below 100 K very similar to the resolution determined elastic intensity, which can be interpreted as the onset of magnetic order, an indirect proof for a change in spin dynamics. In contrast, for low Q, the inelastic intensity, integrated outside of the resolution wing over the energy range within 1.5–5 μeV, runs near $T = 90$ K through a maximum with decreasing temperature and then levels off around $T = 40$ K. This temperature dependence of the inelastic intensity, most clearly seen at the lowest $Q = 0.19$ Å^{-1}, is well known to be a signature of a quasielastic signal which broadens with temperature. The maximum appears at the temperature where the quasielastic signal has its maximum spectral weight within the fixed observation window (see, e.g., Ref. [25]). Very similar but less pronounced behavior is seen for $Q = 0.29$ Å^{-1} and at higher Q, shown for $Q = 0.44$ Å^{-1} where no maximum but a steplike inelastic intensity increase is detected. Thus we conclude that we observe electronic spin fluctuations on the "ns timescale" at low Q, corresponding to larger distances, which are still visible as quasielastic scattering below T_{sf} and which slow down with decreasing temperature. At higher Q, the inelastic intensity does not show a maximum but still a steplike increase, which could mean that at a more local scale the fluctuations are much faster than nanoseconds and slow down at T_{sf}. Therefore, we might expect in principle as well spin dynamics in the high Q range and freezing into diffuse elastic scattering, similar to what has been observed earlier for a frustrated antiferromagnet [26] on IN16.

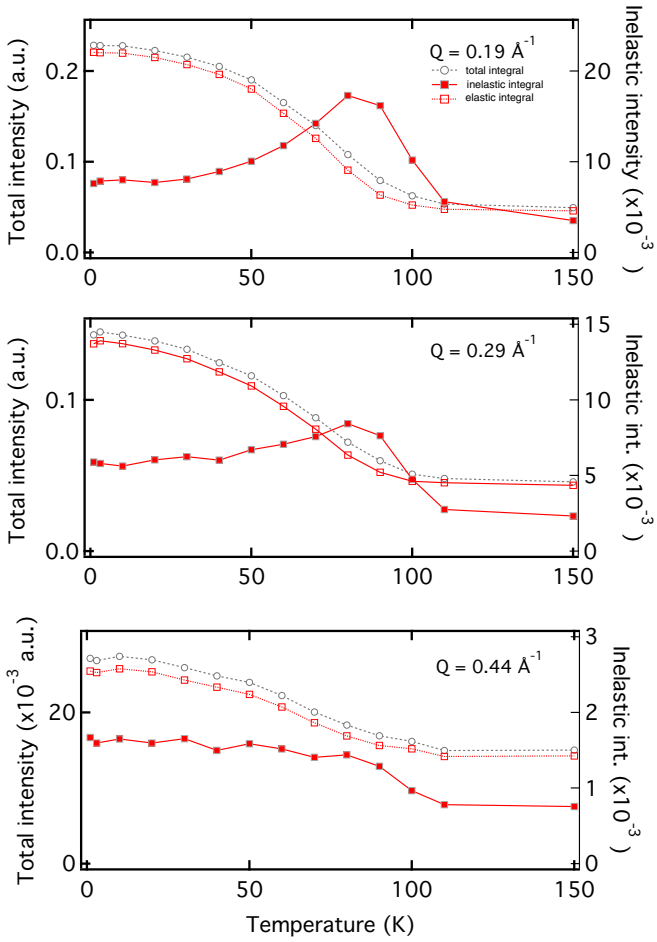

FIG. 14. Temperature dependence of integrated intensities for $SrLaFeCoO_6$ as deduced from IN16B spectra [10] measured over ± 5 μeV for three low Q values. The T-dependence of the inelastic scattering evidences the freezing of spin fluctuations near T_{sf}.

APPENDIX B: La_2FeCoO_6

For the magnetically ordered system La_2FeCoO_6 we have shown in Fig. 11 the existence of an additional Bragg peak at low temperatures. The efws for La_2FeCoO_6 in Fig. 15 shows how this additional Bragg peak develops continuously with decreasing temperature near $Q \approx 1.4$ Å^{-1} within the low Q shoulder of the $Q = 1.61$ Å^{-1} Bragg peak.

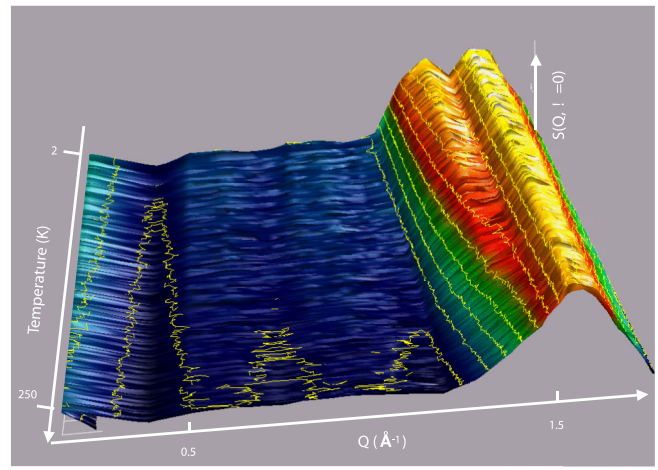

FIG. 15. Elastic intensity of La_2FeCoO_6 as a function of temperature (increasing from back to front) and Q as measured on IN16B. The maximum intensity at the right hand side corresponds to a Bragg peak at $Q \approx 1.61$ Å^{-1} and in cooling below $T = 225$ K its shoulder at the low Q side develops into a further Bragg peak (011) near $Q \approx 1.4$ Å^{-1}.

[1] A. Heidemann, Z. Phys. **238**, 208 (1970).

[2] A. Heidemann, Z. Phys. B **20**, 385 (1975).

[3] A. Heidemann and B. Alefeld, V. IAEA *Symp. Inelastic Neutron Scattering, Grenoble 1972*, IAEA-SM-155/G-4.

[4] T. Chatterji and B. Frick, Physica B **276-278**, 252 (2000).

[5] T. Chatterji, J. Combet, B. Frick, and A. Szyula, J. Magn. Magn. Mater. **324**, 1030 (2012).

[6] T. Chatterji, J. Wuttke, and A. P. Sazonov, J. Magn. Magn. Mater. **322**, 3148 (2010); T. Chatterji and G. J. Schneider, J. Phys.: Condens. Matter **21**, 436008 (2009).

[7] T. Chatterji and N. Jalarvo, J. Phys.: Condens. Matter **25**, 156002 (2013).

[8] T. Chatterji, N. Jalarvo, C. M. N. Kumar, Y. Xiao, and T. Brückel, J. Phys.: Condens. Matter **25**, 286003 (2013).

[9] G. Ehlers, E. Mamontov, M. Zamponi, K. C. Kam, and J. S. Gardner, Phys. Rev. Lett. **102**, 016405 (2009).

[10] See Supplemental Material at http://link.aps.org/supplemental/10.1103/PhysRevB.98.094429 for further details of the high-resolution inelastic neutron scattering study of the nuclear hyperfine splitting and the experimental procedure. Also included are the data treatment and the fit procedures used and the resulting figures.

[11] J. Colmenero, R. Mukhopadhyay, A. Alegria, and B. Frick, Phys. Rev. Lett. **80**, 2350 (1998).

[12] M. García-Hermández, J. L. Martínez, M. J. Martínez-Lope, M. T. Casais, and J. A. Alonso, Phys. Rev. Lett. **86**, 2443 (2001)

[13] J. P. Carlo, J. P. Clancy, T. Aharen, Z. Yamani, J. P. C. Ruff, J. J. Wagman, G. J. Van Gastel, H. M. L. Noad, G. E. Granroth, J. E. Greedan, H. A. Dabkowska, and B. D. Gaulin, Phys. Rev. B **84**, 100404 (2011).

[14] Y. Du, Z. X. Cheng, S. X. Dou, X. L. Wang, H. Y. Zhao, and H. Kimura, Appl. Phys. Lett. **97**, 122502 (2010).

[15] N. S. Rogado, J. Li, A. W. Sleight, and M. A. Subramanian, Adv. Mater. **17**, 2225 (2005)

[16] R. Pradheesh, H. S. Nair, C. M. N. Kumar, J. Lamsal, R. Nirmala, P. N. Santhosh, W. B. Yelon, S. K. Malik, V. Sankaranarayanan, and K. Sethupathi, J. Appl. Phys. **111**, 053905 (2012).

[17] R. Pradheesh, H. S. Nair, V. Sankaranarayanan, and K. Sethupathi, Eur. Phys. J. B **85**, 260 (2012)

[18] R. Pradheesh, H. S. Nair, G. R. Haripriya, A. Senyshyn, T. Chatterji, V. Sankaranarayanan and K. Sethupathi, J. Phys.: Condens. Matter **29**, 095801 (2017).

[19] R. Pradheesh, C. M. N. Kumar, G. R. Haripriya, L. M. Martinez, C. L. Caiz, S. S. Rao, T. Chatterji, V. Sankaranarayanan, K. Sethupathi, and H. S. Nayer (unpublished).

[20] J. Wuttke, A. Budwig, M. Drochner, H. Kämmerling, F.-J. Kayser, H. Klienes, V. Ossovyi, L. C. Pardo, M. Prager, D. Richter, G. J. Schneider, H. Schneider, and S. Staringer, Rev. Sci. Instrum. **83**, 075109 (2012).

[21] http://www.ill.eu/instruments-support/instruments-groups/instruments/in16b/characteristics/ as well as B. Frick, M. Appel, T. Seydel, L. van Eijck, and D. Bazzoli (unpublished).

[22] ILL experiment carried out under doi:10.5291/ILL-DATA.4-04-482.

[23] M. Appel and B. Frick, Rev. Sci. Instrum. **88**, 036105 (2017).

[24] LAMP standard ILL data evaluation software.

[25] B. Frick, J. Combet, and L. van Eijck, Nucl. Instrum. Methods A **669**, 7 (2012).

[26] C. Mondelli, H. Mutka, B. Frick, and C. Payen, Physica B **266**, 104 (1999)

[27] H.-R. Fuh, K.-C. Weng, C.-R. Chang, and Y.-K. Wang, J. Appl. Phys. **117**, 17B902 (2015).

[28] H. Labrim, A. Jabar, A. Belhaj, S. Ziti, L. Bahmad, L. Laanab, and A. Benyoussef, J. Alloys Compd. **641**, 37 (2015).